

Elastic and Inelastic Scattering of  $C^{12}$  by  $C^{12}$  at 127 MeV\*K. H. WANG, S. D. BAKER,<sup>†</sup> AND J. A. MCINTYRE  
Yale University, New Haven, Connecticut

(Received February 26, 1962)

An experimental survey has been made of the elastic and inelastic scattering of  $C^{12}$  by  $C^{12}$  at a laboratory energy of 127 MeV. Inelastic scattering is found to occur for (1)  $Q = -4.4$  MeV (exciting the 4.4-MeV level of  $C^{12}$ ), (2)  $Q = -9.1 \pm 0.3$  MeV [a combination of (a) exciting the 9.65-MeV level of  $C^{12}$  and (b) exciting both  $C^{12}$  nuclei to their 4.4-MeV levels], (3)  $Q = -14.0 \pm 0.5$  MeV (exciting the 14.05-MeV level of  $C^{12}$ ), and (4) possibly  $Q = -19 \pm 1$  MeV (exciting a level, or levels near 19 MeV). Angular distributions of the elastically and inelastically scattered  $C^{12}$  nuclei have been obtained between  $14^\circ$  and  $39^\circ$  in the center-of-mass system. The elastic and  $Q = -4.4$  MeV inelastic distributions show large oscillations which are out of phase in agreement with Blair's phase rule. The  $Q = -14$  MeV distribution, on the other hand, has no oscillations larger than a maximum to minimum ratio of 1.5 to 1.

## I. INTRODUCTION

THE study of the scattering of nuclear projectiles by carbon is attractive experimentally because of the widely spaced energy levels of the  $C^{12}$  nucleus. In addition, the particular case of the  $(C^{12}+C^{12})$  system is of special interest since it has been shown to possess unexpected resonance properties.<sup>1</sup> For these reasons, a survey study of the elastic and inelastic scattering of  $C^{12}$  by  $C^{12}$  has been carried out at a laboratory energy of 127 MeV. A brief report of the early phases of this work has already been published.<sup>2</sup>

## II. EXPERIMENTAL APPARATUS

A schematic diagram of the experimental apparatus is shown in Fig. 1. Except for minor changes, the apparatus has been described before in detail.<sup>3</sup> The beam of  $C^{12}$  ions enters the scattering chamber at the left and is scattered by a 1-mg/cm<sup>2</sup>  $CH_2$  foil, the scattered ions then passing out of the scattering chamber through a window. The scattered ions pass through a second window and into the counting chamber where they are detected by a solid-state detector. The thickness of the two windows plus air path is equivalent to 6.6-mg/cm<sup>2</sup> of Mylar. The pulses from the detector are amplified by a low-noise preamplifier<sup>4</sup> and analyzed on a 400-channel analyzer.<sup>5</sup> As seen in Fig. 1, the scattering chamber has a larger radius (20 in.) over a considerable range of angles, so that the multiple scattering of the scattered ion by the exit window will not affect the angular resolution of the detector. The energy of the  $C^{12}$  ion beam

was determined by range measurements using the range-energy data of Northcliffe.<sup>6</sup>

The data were taken with the 400-channel analyzer, the analyzer being gated by a single-channel analyzer which detected all pulses above a fixed discriminator level. The counts from the fast single-channel analyzer were used for the cross-section calculation. The cross sections for the various peaks appearing on the 400-channel analyzer were determined by taking ratios between the areas of the peaks compared to the total area under the pulse-height spectrum, the area being normalized to the single-channel analyzer. This procedure circumvented the necessity for considering the effects of the long dead time ( $\sim 100$   $\mu$ sec) of the 400-channel analyzer. The absolute cross section was determined by measuring the elastic scattering from  $Au^{197}$  target at small angles where Rutherford scattering is known to occur. By assuming that the cross section so measured was the Rutherford cross section and knowing the thickness of the  $Au^{197}$  target, the Faraday cup efficiency and counter solid angle were determined. These quantities, coupled with the knowledge of the  $CH_2$  target thickness, permitted the calculation of the  $C^{12}$  scattering cross sections. It is believed that the absolute cross sections are accurate to  $\pm 20\%$  while the relative cross sections between the elastic and inelastic  $C^{12}$  scatterings are accurate to  $\pm 5\%$ .

The particle identification and the energy determination of the detected ions were achieved by recording the pulse-height spectrum of the detector both with, and without, a 12.55-mg/cm<sup>2</sup> aluminum degrading foil

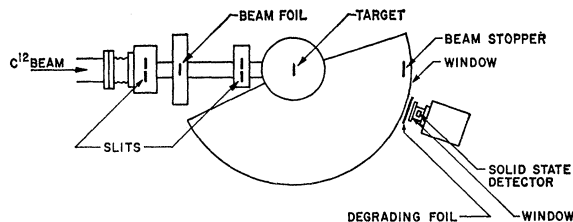


FIG. 1. Schematic diagram of the scattering apparatus.

\* L. C. Northcliffe, Phys. Rev. **120**, 1744 (1960).

\* Supported by the U. S. Atomic Energy Commission.

<sup>†</sup> Raytheon Predoctoral Fellow in Physics, 1960-1961.<sup>1</sup> D. A. Bromley, J. A. Kuehner, and E. Almqvist, Phys. Rev. Letters **4**, 365 (1960); D. A. Bromley, J. A. Kuehner, and E. Almqvist, Phys. Rev. **123**, 878 (1961).<sup>2</sup> S. D. Baker, K. H. Wang, and J. A. McIntyre, *Proceedings of the International Conference on Nuclear Structure, Kingston, 1960* (University of Toronto Press, Toronto, 1960), p. 926.<sup>3</sup> J. A. McIntyre, S. D. Baker, and K. H. Wang, Phys. Rev. **125**, 584 (1962).<sup>4</sup> We are indebted to E. R. Beringer for providing us with the preamplifier.<sup>5</sup> Radiation Instrument Development Laboratory, Inc., 61 East North Avenue, Northlake, Illinois.

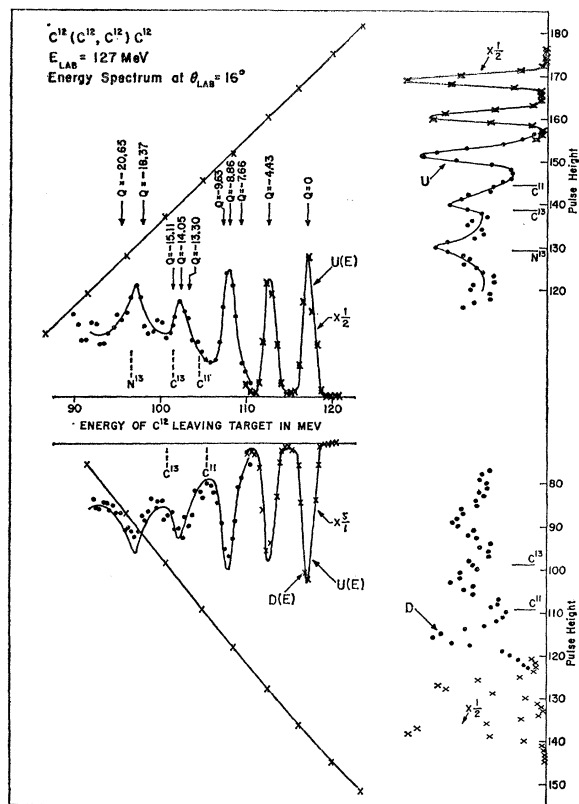


FIG. 2. Display of the particle identification and energy calibration technique. The upper right vertical spectrum was taken experimentally without the degrading foil and is denoted  $U$  (undegraded). It is reflected on the calibration curve at the upper left to give the erect  $C^{12}$  energy spectrum at the target  $U(E)$ . The lower right vertical spectrum was taken experimentally with the degrading foil and is labelled  $D$  (degraded). These points are reflected on the calibration curve at the lower left to give the points of the inverted horizontal spectrum,  $D(E)$ . The curve of the inverted spectrum is the reflection through a horizontal axis of the erect (undegraded)  $U(E)$  spectrum. The  $C^{11}$ ,  $C^{13}$ , and  $N^{13}$  lines show how peaks corresponding to these nuclei would be shifted between the erect and inverted spectra while  $C^{12}$  peaks should be unshifted.

placed outside the scattering chamber between the detector and the target (see Fig. 1). The effect of this foil was such as to shift the energies of  $C^{11}$  and  $C^{13}$  nuclei striking the detector by about 1.4 MeV with respect to the energies of  $C^{12}$  nuclei striking the detector; this effect depended on the difference of  $dE/dx$  for the  $C^{11}$ ,  $C^{12}$ , and  $C^{13}$  nuclei in the degrading foil.  $B^{11}$  and  $N^{13}$  nuclei, on the other hand, were shifted, respectively, by 7 and 10 MeV. With this absorption technique, the identification of the  $C^{12}$  nuclei could be obtained.

The detector pulse height was calibrated against the  $C^{12}$  energy at the target by the following method. A thin gold target was placed in the  $C^{12}$  beam and the elastic scattering peak from the solid-state detector was located on the 400-channel analyzer. The pulse height corresponding to this peak was then considered to be associated with the known scattered energy at the target of the  $C^{12}$  ions. An absorber foil (the beam foil in Fig. 1)

was then placed in the  $C^{12}$  beam thereby reducing the beam energy, and the elastic scattering peak again located on the 400-channel analyzer. This measurement produced a second relationship between detector pulse height and the energy for  $C^{12}$  ions leaving the target. A series of similar measurements then generated a curve relating detector pulse height to  $C^{12}$  energy leaving the target. A second curve relating  $C^{12}$  energy at the target to detector pulse height was generated in a similar manner with the degrading foil added between the detector and the target. Detector pulse-height information obtained both with and without degrading foil could then be converted to the energy of  $C^{12}$  nuclei leaving the target. With these calibration curves, the energy of  $C^{12}$  nuclei leaving the target could be determined from a pulse-height measurement without needing to know the energy loss of the  $C^{12}$  nuclei in the window.

The conversion to an energy scale of detector pulse-height data obtained by scattering 127-MeV  $C^{12}$  nuclei from  $C^{12}$  nuclei is illustrated in Fig. 2. Plotted vertically at the right are the pulse-height spectra obtained on the 400-channel analyzer; the upper spectrum (denoted by  $U$ , for undegraded) was obtained without the degrading foil between the detector and the target, the lower spectrum (denoted by  $D$ , for degraded) was obtained with the degrading foil in place. Notice should be taken that the lower scale increases in the downward direction. A line connecting the experimental points has been drawn on the  $U$  (undegraded) spectrum. Next, the two calibration curves previously discussed are plotted in Fig. 2 at the upper and lower left. The pulse-height spectrum  $U$  at the upper right is then reflected from the curve at the upper left and the energy spectrum of the  $C^{12}$  ions leaving the target is obtained (if the detected ions are indeed  $C^{12}$ ). This spectrum is the erect horizontal spectrum  $U(E)$ . The check on whether the detected ions are indeed  $C^{12}$  is obtained as follows. The lower pulse-height distribution  $D$ , obtained with the degrading foil (consisting only of points in Fig. 2), is reflected from its calibration curve at the lower left and an energy spectrum  $D(E)$  from the degraded pulse-height distribution is obtained. This spectrum, consisting only of points, which appears upside down is again an energy spectrum of the  $C^{12}$  leaving the target and so should be identical with the first (erect) energy spectrum obtained  $U(E)$ , if the detected ions are  $C^{12}$ . To check the identity of the two spectra, the curve of the undegraded spectrum  $U(E)$  is reflected through a horizontal axis onto the spectrum of points  $D(E)$  and it is this reflected curve  $U(E)$  that is seen to be lying on the points of the degraded spectrum  $D(E)$ . It is clear that the fit between the independently obtained energy spectrum curve  $U(E)$  and the points  $D(E)$  is excellent for most of the spectrum, thereby proving that the spectrum is a  $C^{12}$  spectrum.

The discrimination of the system against the  $C^{11}$  and  $C^{13}$  isotopes as well as against the  $N^{13}$  nucleus is indi-

cated by the dashed lines on the energy scale. In the upper, undegraded energy spectrum  $U(E)$ , the positions of the  $C^{11}$  and  $C^{13}$  lines are those expected for the reaction  $C^{12}(C^{12}, C^{11})C^{13}$  going to the ground states of the two isotopes, while the  $N^{13}$  line corresponds to the  $C^{12}(C^{12}, N^{13})B^{11}$  ground-state reaction. In the lower energy spectrum the positions of the  $C^{11}$  and  $C^{13}$  lines are seen to be shifted by 1.4 MeV with respect to the upper energy spectrum. Thus, if a  $C^{11}$  peak occurred in the upper spectrum, its position would be shifted 1.4 MeV in the lower spectrum and it would not be identified as a  $C^{12}$  peak. The spectra show that a  $C^{13}$  peak would also shift about 1.4 MeV while the  $N^{13}$  peak has been shifted off the diagram. The method used for locating the  $C^{11}$ ,  $C^{13}$ , and  $N^{13}$  lines on the energy spectra is described in an Appendix.

### III. DISCUSSION OF RESULTS

The energy spectrum shown in Fig. 2 is typical of those obtained for laboratory scattering angles between  $7^\circ$  and  $19^\circ$ . As reported earlier,<sup>2</sup> sharp peaks are seen to be present for the elastic scattering, and for inelastic scattering with  $Q = -4.4$ ,  $-9$ , and  $-14$  MeV. Also prominent in the spectrum shown in Fig. 2 is a peak at  $Q = -19$  MeV.

#### A. Elastic Scattering and the 4.4-MeV Peaks

There is no doubt that the 4.4-MeV peak arises from excitation of the 4.43-MeV level in one of the  $C^{12}$  nuclei by the inelastic scattering process. Angular distributions

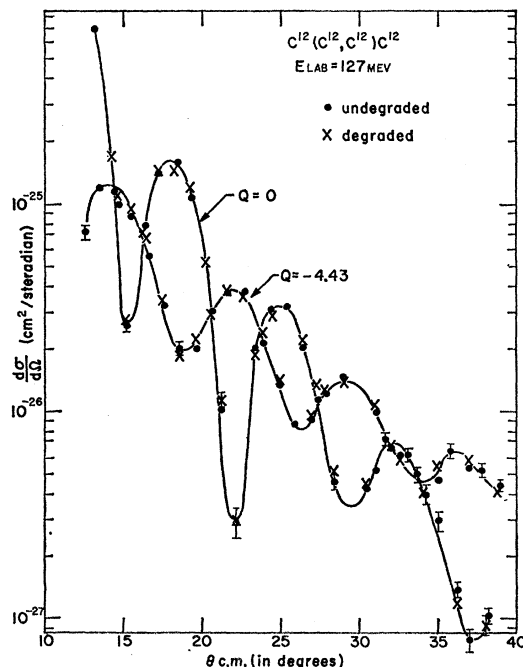


FIG. 3. Angular distributions for the elastic scattering of  $C^{12}$  by  $C^{12}$  and the inelastic scattering for  $Q = -4.4$  MeV.

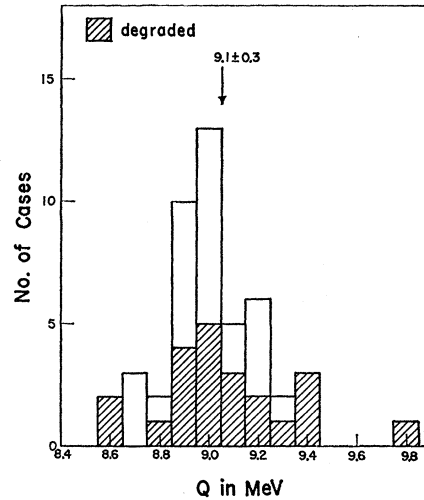


FIG. 4. Histogram showing the number of "9-MeV" peaks found at various  $Q$  values.

of the elastic peak and the 4.4-MeV peak are shown plotted in Fig. 3. The  $\bullet$  and  $\times$  points correspond to data taken with undegraded and degraded detection; the agreement between these two methods indicates that the introduction of the degrader does not affect the  $C^{12}$  peaks. The striking features of the curves in Fig. 3 are their large oscillations and the fact that the 4.43-MeV curve is out of phase with the elastic curve. The large oscillations are typical for heavy-ion elastic scattering<sup>7</sup> with  $\eta = ZZ'e^2/\hbar v < 5$ , and the out-of-phase inelastic scattering is in agreement with Blair's phase rule,<sup>8</sup> that inelastic scattering to even parity states should be out of phase with the elastic scattering. These features were pointed out in the preliminary report of this work<sup>2</sup> and were subsequently found to be present at smaller scattering angles by Smith and Steigert<sup>9</sup> and by Williams and Steigert.<sup>10</sup>

#### B. The 9-MeV Peak

The identification of this peak as a  $C^{12}$  peak is made by the type of measurements exhibited in Fig. 2. The  $Q$ -value determination of the peak can be made by locating the center of the peak for each angle studied. The histogram in Fig. 4 shows the number of cases obtained for various  $Q$  values. The shaded areas correspond to  $Q$  measurements taken with the degrading foil between the detector and the target. Since the mean  $Q$  value for the degraded cases is close to that for the undegraded cases, the 9-MeV peak is due to  $C^{12}$  nuclei. The mean  $Q$  value for the peak is found to be  $9.1 \pm 0.3$  MeV.

<sup>7</sup> J. A. McIntyre, S. D. Baker, and T. L. Watts, Phys. Rev. **116**, 1212 (1959).

<sup>8</sup> J. S. Blair, Phys. Rev. **115**, 928 (1959).

<sup>9</sup> A. M. Smith and F. E. Steigert, Phys. Rev. **125**, 988 (1962).

<sup>10</sup> D. J. Williams and F. E. Steigert, Nuclear Phys. (to be published).

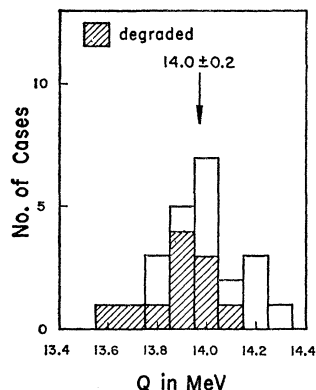


FIG. 5. Histogram showing the number of "14-MeV" peaks found at various  $Q$  values.

The inelastic scattering processes accounting for this peak cannot be determined however, because there are several processes which would yield  $C^{12}$  peaks near a  $Q$  value of  $-9$  MeV. These processes are the following: (1) excitation of one  $C^{12}$  nucleus to its 7.65-MeV level, (2) excitation of one  $C^{12}$  nucleus to its 9.65-MeV level, or (3) excitation of both  $C^{12}$  nuclei to their 4.43-MeV levels ( $Q = -8.86$  MeV). From the histogram of Fig. 4, and taking into account the fact that some of the 9-MeV peaks are appreciably broader than the experimental linewidth, the following conclusions have been drawn: (1) Excitation of the 7.65-MeV level is negligible at all angles (less than 10% of the peak), (2) The double excitation ( $Q = -8.86$  MeV) and the 9.65-MeV excitation are comparable in magnitude over the range of angles studied.

The uncertainty concerning the contribution of the double excitation process to the peak has been removed recently by Garvey, Smith, Hiebert, and Steigert<sup>11</sup> who circumvent the whole resolution problem ingeniously by detecting the scattered and recoil  $C^{12}$  nuclei in coincidence. Since the  $C^{12}$  nucleus excited to 9.65 MeV is alpha-particle unstable, inelastic scattering events exciting the 9.65-MeV level will not produce coincidences, while inelastic events exciting both  $C^{12}$  nuclei to 4.43 MeV will produce coincidences. The angular distribution for the double excitation has been obtained by Garvey *et al.*<sup>11</sup> for center-of-mass angles from  $27^\circ$  to  $42^\circ$ .

### C. 14-MeV Peak

The identification of this peak as a  $C^{12}$  peak must be performed carefully because of the presence of  $C^{11}$  and  $C^{13}$  nuclei having energies close to the  $C^{12}$  energy. For the laboratory angles between  $11^\circ$  and  $16^\circ$  the  $Q$  value of the 14-MeV peak was determined from its position in the energy spectrum, for both the undegraded and degraded detection arrangement. The number of cases of a particular  $Q$  value vs  $Q$  value is plotted in Fig. 5. The shaded areas correspond to the degraded detection arrangement, the unshaded areas to undegraded detec-

tion. There is no systematic shift between the unshaded and shaded areas, of greater than 0.1 MeV. This result identifies the peak as a  $C^{12}$  peak since a  $C^{11}$  or  $C^{13}$  peak would shift 1.4 MeV between the degraded and undegraded situation.

The histogram in Fig. 5 also identifies the energy level excited in the  $C^{12}$  nucleus as the 14.05-MeV level, since the neighboring known  $C^{12}$  levels of 13.3 and 15.1 MeV are far enough removed to be eliminated from consideration. While the width of the histogram is only  $\pm 0.2$  MeV, some allowance should be made for error in energy calibration so that the  $C^{12}$  energy level is determined here to be  $14.0 \pm 0.5$  MeV.

Garvey *et al.*<sup>11</sup> have pointed out that a two-phonon excitation of one  $C^{12}$  nucleus would produce an energy level near 15 MeV. Lemmer, de-Shalit, and Wall<sup>12</sup> have shown in the Born approximation that such two-phonon excitations would yield inelastic scattering angular distributions with oscillations in phase with the elastic scattering oscillations. It would be interesting therefore to measure the angular distribution of the 14-MeV peak to determine whether the scattering is consistent with a two-phonon excitation of the 14.05-MeV level in  $C^{12}$ . An attempt has been made to make this measurement but the large skew background under the 14-MeV peak makes an accurate determination of the magnitude of the 14-MeV peak difficult. Allowing a large uncertainty for the magnitude of the background under the peak an

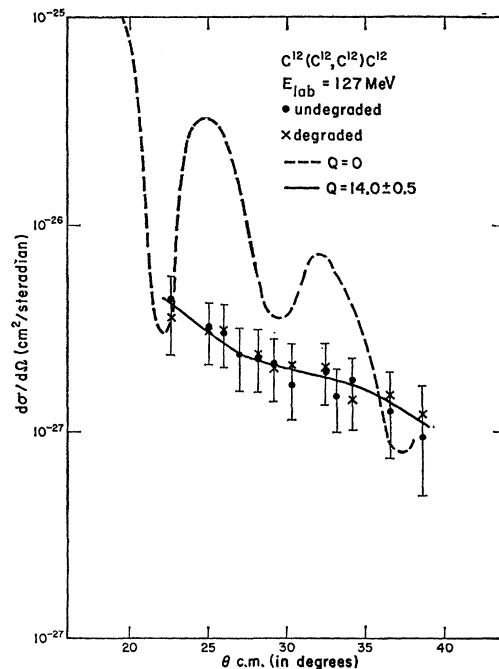


FIG. 6. Angular distribution for the inelastic scattering of  $C^{12}$  by  $C^{12}$  for  $Q = -14$  MeV. The dashed curve is the experimentally determined elastic scattering distribution (see Fig. 3).

<sup>11</sup> G. T. Garvey, A. M. Smith, J. C. Hiebert, and F. E. Steigert, Phys. Rev. Letters **8**, 25 (1962).

<sup>12</sup> R. H. Lemmer, A. de-Shalit, and N. S. Wall, Phys. Rev. **124**, 1155 (1961).

angular distribution was obtained and is plotted in Fig. 6. The cross section drops slowly with angle as predicted by Lemmer *et al.*<sup>12</sup> However, because of the large uncertainties assigned to each of the points, no information is obtained about the oscillation of the cross section with angle except that the oscillations are less than 1.5 to 1 in their magnitude.

#### D. 19-MeV Peak

This peak has appeared at most of the larger angles but is not always sharp. At a few angles its width is consistent with the excitation of only one energy level in  $C^{12}$ , yet the close level spacing ( $\sim 0.3$  MeV) makes it impossible to prove that only one level is excited. Inspection of Fig. 2 shows that the *points* on the inverted energy spectrum lie above the *curve* on the inverted spectrum in the 19-MeV peak so that some of the peak is not produced by  $C^{12}$ . It is possible, in fact, that all of the peak is made up of  $C^{11}$  and  $C^{13}$  in such excited states as to yield a  $Q$  value corresponding to the 19-MeV peak. The present measurements are not definitive concerning the identity of the nuclei producing this peak. If the peak is  $C^{12}$  it corresponds to an energy of excitation of  $19 \pm 1$  MeV.

#### IV. CONCLUSIONS

The elastic and inelastic scattering of  $C^{12}$  by  $C^{12}$  have been studied at laboratory scattering angles from 7 to  $19^\circ$ . Energy spectra of the scattered  $C^{12}$  nuclei have shown five prominent peaks, an elastic scattering peak, and four inelastic scattering peaks with  $Q$  values corresponding to  $-4.4$ ,  $-9$ ,  $-14.0$ , and  $-19$  MeV. The 4.4-MeV peak and 14.0-MeV peak are consistent with the excitation of one  $C^{12}$  nucleus to the known energy levels 4.43 and 14.05 MeV. Garvey *et al.*<sup>11</sup> have shown that some of the 9-MeV peak is due to excitation of both  $C^{12}$  nuclei to the 4.43-MeV level. The remainder of the peak comes from excitation of one  $C^{12}$  nucleus to the 9.65-MeV level. The 19-MeV peak seems to have some contribution, which may be large, from nuclei other than  $C^{12}$ . Angular distributions of the elastic and 4.4-MeV inelastic peaks show that the elastic and 4.4-MeV inelastic oscillations are out of phase as expected according to the Blair phase rule. On the other hand, the 14.0-MeV inelastic angular distribution shows no oscillations although oscillations of magnitude less than 1.5 to 1 would not be revealed by the present measurements.

#### ACKNOWLEDGMENTS

We are indebted to G. K. Tandon for assistance with the measurements and data analysis. We have also profited from discussions with G. T. Garvey about the

double excitation contribution to the 9-MeV peak. Finally, we wish to thank L. Baron and the accelerator crew for the  $C^{12}$  beams used.

#### APPENDIX

The locations of the  $C^{11}$  and  $C^{13}$  peaks on the upper and lower energy spectra of Fig. 2 were obtained as follows.

(1) The  $Q$ -value calculation for the reaction  $C^{12}(C^{12}, C^{13})C^{11}$  gave the energies of the  $C^{11}$  and  $C^{13}$  nuclei leaving the target. Similar calculations gave the energies of the  $C^{12}$  nuclei leaving the target for the various inelastic scattering possibilities.

(2) Using the range-energy data for carbon ions in Mylar<sup>13</sup> and the window thickness of  $6.6 \text{ mg/cm}^2$ , the "energies of the  $C^{12}$  nuclei at the detector" were calculated and plotted as a curve against " $C^{12}$  energies leaving the target." Combining this curve with the calibration curve of "detector pulse height" vs " $C^{12}$  energy at the target" (the curve at the upper left of Fig. 2), a curve of "detector pulse height" vs " $C^{12}$  energy at the detector" was obtained. This curve proved to be linear, in agreement with the expected response of solid-state detectors,<sup>14</sup> thereby checking the validity of the energy loss calculation for the window. A similar curve was obtained for the situation of the degrading foil being in position.

(3) With the pulse height of the detector calibrated in terms of detector energy, the pulse heights of  $C^{11}$  and  $C^{13}$  nuclei striking the detector could be calculated for the  $C^{12}(C^{12}, C^{11})C^{13}$  reaction for both the undegraded and the degraded situations. These pulse heights are indicated by lines on the vertical spectra at the right of Fig. 2. This means that, if  $C^{11}$  and  $C^{13}$  nuclei were produced in the target, pulse-height peaks would occur in the spectra at the positions of these lines.

(4) The vertical spectra were then reflected in the calibration curves shown at the left of Fig. 2. The positions of the  $C^{11}$  and  $C^{13}$  lines so reflected are shown as dashed lines in the horizontal spectra.  $C^{11}$  and  $C^{13}$  peaks would appear at the positions of the dashed lines. It is seen that the position of each of the dashed lines has shifted about 1.4 MeV between the upper and lower horizontal spectra. Thus, if  $C^{11}$  and  $C^{13}$  peaks had appeared, they would have shifted about 1.4 MeV in their positions between the upper and lower spectra and could thereby be identified. (Note that the shift is in the opposite direction for the  $C^{11}$  and  $C^{13}$  peaks.)

<sup>13</sup> P. E. Schambra, A. M. Rauth, and L. C. Northcliffe, *Phys. Rev.* **120**, 1758 (1960).

<sup>14</sup> A. E. Larsh, G. E. Gordon, and T. Sikkeland, *Rev. Sci. Instr.* **31**, 1114 (1960).